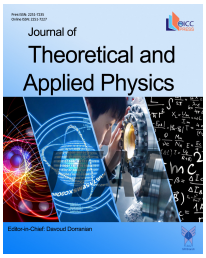

Volume 17, Issue 5, 172349 (1-7)

Journal of Theoretical and Applied Physics (JTAP)

https://dx.doi.org/10.57647/j.jtap.2023.1705.49

Magneto-plasmonic properties of hybrid nanostructures prepared by laser ablation in different solutions

Rashiid Ali Ejbarah[1], Ahmed Kadem Kodeary[2]*, Talib M. Abbas[3]

[1]*Department of Petroleum and Gas Engineering, College of Engineering, University of Thi-Qar, Iraq.*
[2]*Department of Laser Physics, College of Science for Woman, University of Babylon, Babylon, Iraq.*
[3]*Physics Department, College of Education for Pure Sciences, University of Babylon, Babylon, Iraq.*

***Corresponding author**: ahmed88k88@yahoo.com

Received 23 June 2023; Accepted 31 July 2023; Published Online 29 August 2023 ORIGINAL RESEARCH

Abstract:
The present experimental study aims to synthesize and evaluate the magneto-plasmonic properties of metallic nanoparticles to introduce a hybrid of core-shell nanoparticle that can be used in biomedical and optical applications. For these core-shell nanoparticles, gold (Au) was used as the plasmonic material and iron (Fe) as the partner in the magnetic parts. The core-shell nanoparticles were prepared by pulsed laser ablation in liquid media using a Nd:YAG pulsed laser in deionized water, as well as an aqueous solution of PVP, and for comparison an aqueous solution of PVA. Furthermore, the plasmonic and magnetic properties of the experimentally prepared core-shell nanoparticles were studied by optical spectroscopy and the vibrating sample magnetometer method within a variable magnetic field of up to 1 T. The results revealed tunable and adjustable optical linear behavior and obvious plasmonic properties by tracking the refractive index under different physical media. The results also showed that Superparamagnetic properties of core/shell nanoparticles were achieved by changing the surrounding medium. Accordingly, the results could open up new insight into the magneto-plasmonic region for beneficial biomedical applications.

Keywords: Laser ablation in Liquids; Magneto-plasmonic properties; Core shell nanoparticles

1. Introduction

Nanoparticles (NPs) and nanostructured materials (NSMs) represent an active research subject and a growing technology industry with applications in a wide range of fields, where their unique phenomena allow for new applications [1]. Thus, since Faraday's pioneering work on experimental reactions of colloidal metal NPs to light in the eighteenth century, the metallic NPs have become the focus of nanoscience and technology due to their amazing physical and chemical properties [2], because these physical and chemical properties of nanomaterials are highly dependent on their sizes and shapes. Therefore, research in this scientific field is directed towards developing simple and efficient methods for fabricating nanomaterials that allow the size and morphology of nanoparticles to be controlled and thus their properties [3].
There has recently been a slew of papers published in the field of nanomaterials that look into the synthesis and properties of magnetic NPs [4]. Interest in these materials stems from the applications of these nanoparticles, ranging from their use in biochemistry [5], targeting of medicine in the body [6], and magnetic electrophoresis of specific biological entities [7], to the use these materials as recording media [8]. Metal oxides, such as different ferrites, are some of the most representative magnetic materials. However, because they are frequently made up of multiple oxides, their magnetic characteristics are not always well-defined and repeatable [9]. Pure metals like cobalt, iron, and nickel, as well as their metal alloys, are also employed in a variety of magnetism applications [10]. The characteristics of these minerals are far more suitable than those of iron oxides [11]. Ferromagnetic behavior is observed in magnetic transition metals with nanostructures, whereas super-magnetic behavior is shown in iron metals [12]. In addition, in the absence of a magnetic field, transition metals retain their magnetic characteristics, whereas iron oxide nanostructures do not [12].
Also, core-shell NPs are a novel class of nanostructures with unique and customized features that are distinct from

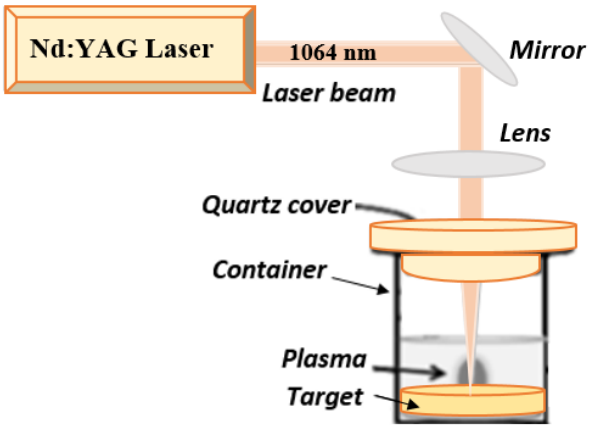

Figure 1. Schematic diagram of nanoparticle preparation by laser ablation method.

their single counterparts and are used in a wide range of applications [13, 14]. Surface plasmon resonance (SPR) and local field enhancement of metals are responsible for the intriguing and peculiar optical features of core-shell metal NPs, which led to their use in optoelectronic devices [15]. The reports categorically show that the core-shell architectures have enhanced magnetic properties than that of single counterparts [16, 17].
In the literature, few recent reports on hybrid nanostructures are available, and there is still a great need for business development efforts from works on ferromagnetic nanostructures, on this basis, the topic of our research has been selected.

2. Samples fabrication: laser ablation in liquids

A pure gold plate (99.99% purity, purchased from Sigma Aldrich, Germany) was placed on the bottom of the beaker with 20 ml of deionized water. A laser with the specifications of (1064 nm repetition of 6 Hz, pulse duration of 50 ns, and pulse energy of 120 mJ) was focused by the reflected mirror on the target of 3×3 mm^2. The Au sample was labeled after ablating the Au plate in deionized water for 3 minutes (Au colloid). Then an iron plate (99.99% purity, purchased from Houston Inc., USA) was ablated by the same laser in the Au colloid solution. The samples of Fe@Au were obtained after ablation for 2 minutes.
Fig. 1 shows a schematic of the experimental setup used to prepare nanoparticles by laser ablation confined to a liquid medium.
The experiment was repeated, but this time the iron target was placed in the deionized water firstly and was exposed to a laser with the same specifications. The Fe sample was labeled after ablating the Fe plate in deionized water for 3 minutes (Fe colloid). Then an Au plate was ablated by the same laser in the Fe colloid solution. The sample of Au@Fe was obtained after the ablation for 2 minutes. The experiment was repeated with all its details except that the deionized water was replaced with a polyvinylpyrrolidone polymer (PVP), and a third time, but this time the deionized water was replaced with a polyvinyl alcohol polymer (PVA). The PVP and the PVA polymers were dissolved in distilled deionized water at a percentage of (1%), in order to increase the stability of nanoparticles in solution. All of the samples were characterized by FE-SEM (JEOL-7601), spectrometer, Ocean 2000 and UV-Vis Homomatsu.

3. Experimental results

3.1 Optical properties

Fig. 2 shows the absorption spectrum of gold and iron nanomaterials separately. The strong interaction with light occurs because the conduction electrons on the surface of the gold metal undergo a collective oscillation when they are excited by light at certain wavelengths. This oscillation is known as surface plasmon resonance, which is why the absorption intensity of gold nanoparticles is much higher than that of similar non-plasmon nanoparticles (Fig. 2(a)). The intensity and wavelength of the SPR band are affected by parameters such as the metal type, particle size, shape, structure, composition, and the dielectric constant of the surrounding medium, all of which affect the electron charge

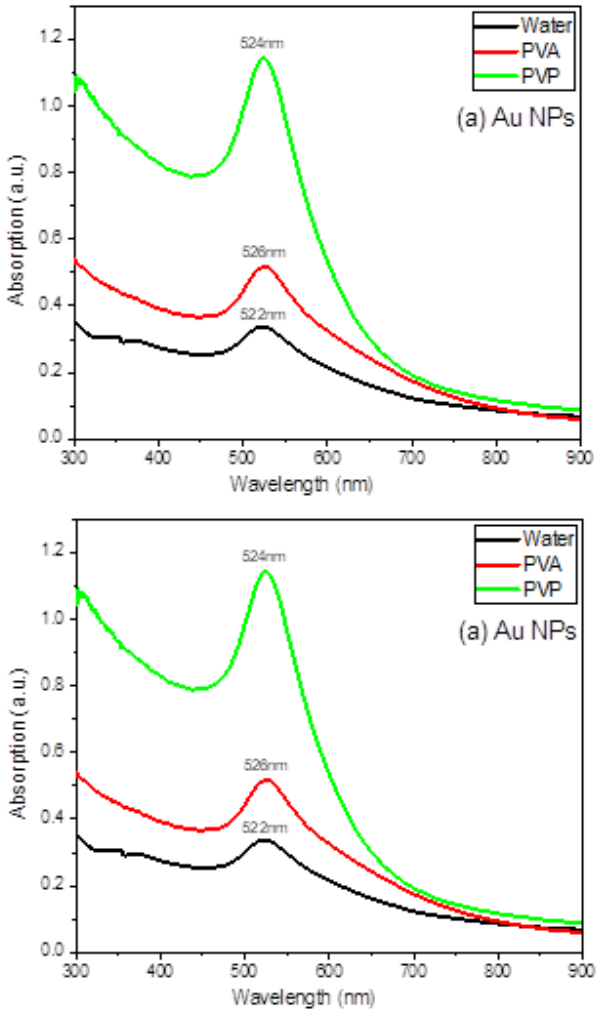

Figure 2. Absorption spectra of: (a) the gold NPs and (b) the iron NPs in deionized water compared to a polymer matrix.

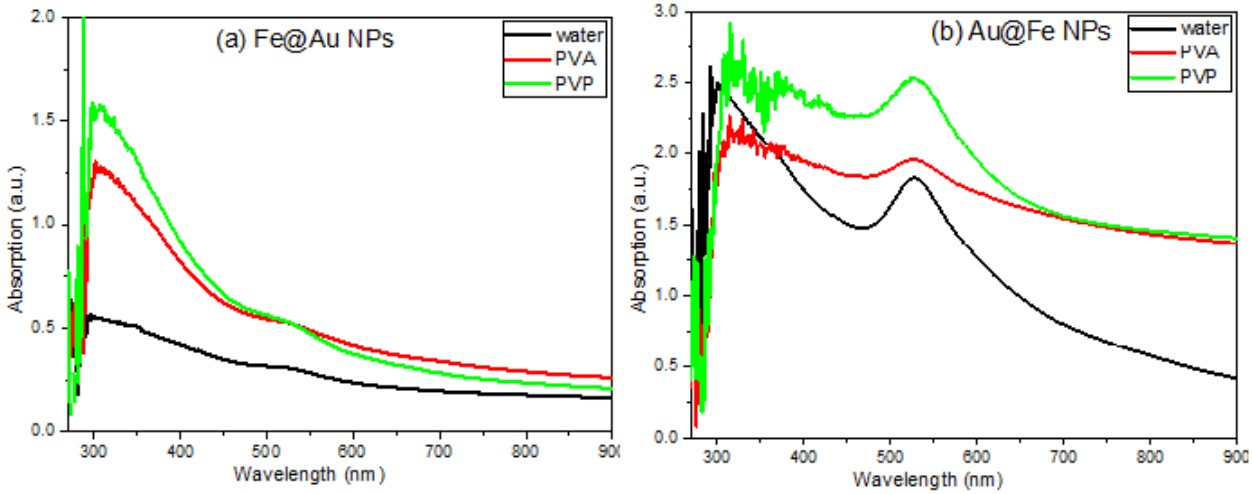

Figure 3. Absorption spectra of: (a) the Fe@Au NPs , and (b) the Au@Fe NPs in the three different solutions.

density on the particle surface. Therefore, the peak absorption of gold nanoparticles in the PVP solution is more obvious because it keeps the nanoparticles suspended and does not allow their sedimentation due to the higher viscosity and higher refractive index than deionized water and PVA solution. Moreover, one can see a redshift in the SPR wavelength (522 – 526 nm) when changing the surrounding medium and this wavelength shift indicates an increase in the size of the nanoparticles when generated by polymer compared to water, which was confirmed in these samples at FE-SEM images. In addition, this redshift due to the larger refractive index of the surrounding medium leads to the modulation of the SPR wavelength of the samples. This red shift when generating nanoparticles in the polymer matrix compared to deionized water is due to the accumulation of more nanoparticles inside the polymer particles, which led to larger particle size and this, in turn, leads to an increase in the refractive index of the medium [18].

The optical absorption of the iron NPs in the wavelength of 190 – 900 nm has been studied. The UV-visible spectra of iron based NPs synthesized by laser ablation in the deionized water, the PVA, and the PVP polymers are shown in (Fig. 2(b)) respectively. In the polymer, the optical absorption of iron nanoparticles increases more than that in deionized water for the same reason mentioned above when discussing gold nanoparticles in the three different media. it is also noticed a redshift in the wavelength in the absorption spectrum of the Fe NPs in the PVA and the PVP solutions respectively (304 – 312 nm) which means the increase in the size of the Fe NPs.

As expected, in the core-shell nanoparticle samples, it can be observed two distinct absorption spectra peaks that come from the absorption of each individual material in the nanostructure indicating the successful formation of the core/shell nanostructure for all samples which is confirmed in (FE-SEM) images (Fig. 3).

Figure 3(a) shows the visible and ultraviolet light absorption spectra of Fe@Au NPs in deionized water solution compared to PVA and PVP solutions. The first two absorption regions in the wavelength (298 – 306 nm) refer to the absorption of iron particles, while the other in the visible region at the wavelength (528 – 533 nm) refers to gold NPs, with the red shift at the top of the absorption spectrum when moving from the aqueous matrix to the polymer matrix due

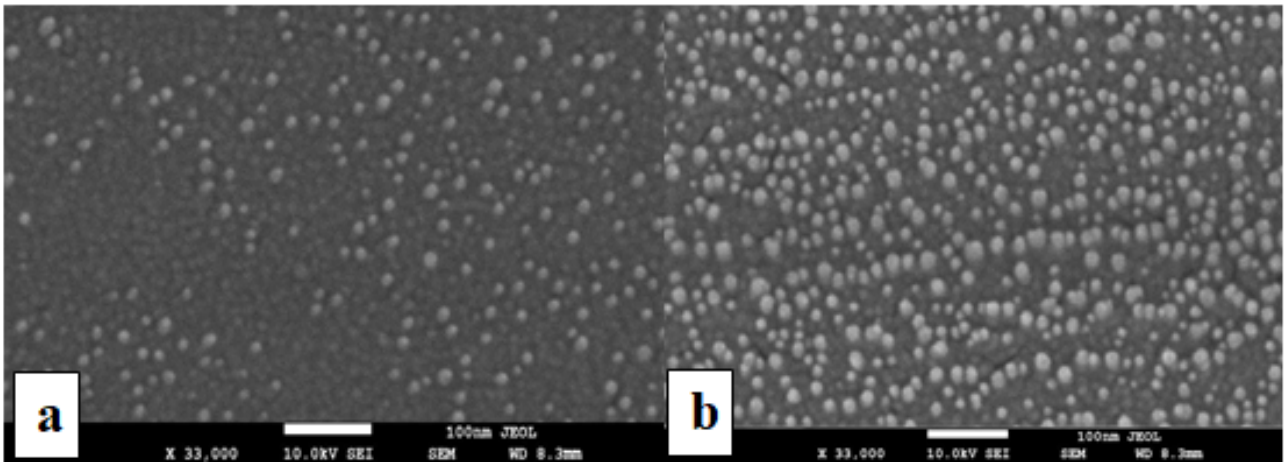

Figure 4. FE-SEM image of Au NPs (a) in the deionized water, (b) in the PVP polymer solution.

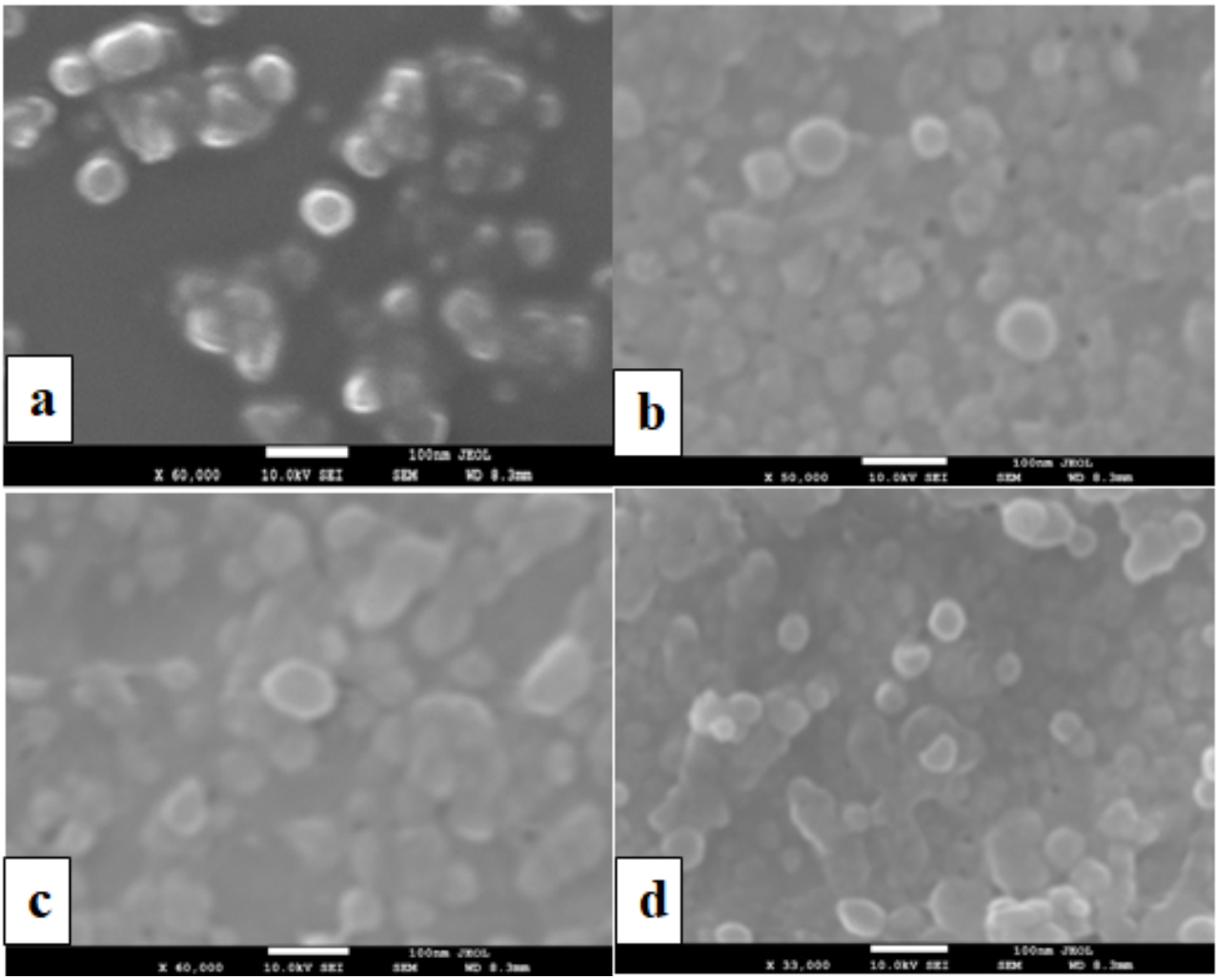

Figure 5. FE-SEM image of the core/shell NPs: (a) Au@Fe in deionized water, (b) Fe@Au in PVA polymeric solution, (c) Au@Fe in PVA polymeric solution, (d) Fe@Au NPs in PVP polymeric solution.

to the aforementioned reason.

In comparison with the optical properties of Fe@Au, Fig. 3(b), represents the optical absorption of Au@Fe in aqueous and polymer solutions. It was observed that two distinct and clear absorption peaks, each denoting the mineral substances in the solution, also it is noticed that the absorption spectrum of Au@Fe in PVP polymer is larger than that of PVA polymer, which in turn is better than in distilled water due to the increase in the refractive index of the solution and the increase in the size of nanoparticles. It is as well evident that the absorption peaks of Au@Fe are more clear and sharp compared to the samples Fe@Au NPs, because of the composition of the sample which made the absorption of Au NPs greater, as it is known that SPR is highly dependent on the shape, size and composition of nanoparticles, and the local SPR position is very sensitive to the refractive index of the medium [19]. Based on the results, we got good control over the optical properties and wavelength shifts that are useful in designing optical devices and instruments. Our results are consistent with other studies [20, 21].

3.2 Morphological properties

The morphology, size, and shape of the samples were examined using an FE-SEM field emission scanning electron microscope as shown in Fig. 4. The average size of the nanomaterial has been calculated using Image J software, and the number of core-shell nanoparticles is selected to take the average core size and shell thickness of the samples in the distilled deionized water and the PVP polymeric solutions. The results showed that the average size of nanoparticles in the PVP polymeric solution increases when compared with the deionized distilled water solution, and this is due to the accumulation of the NPs inside the polymer, and our results are supported by [22, 23].

It is noticed from the results that all the nanoparticles that were produced by the method of laser ablation are spherical in shape. The results also showed that the average size of the Au NPs in the distilled water solution is 17 nm (see Fig. 4(a)) as expected, the average size of the Au NPs increased to 24 nm when they were created in PVP (see Fig. 4(b)). For the core-shell NPs formed as spheroids with the core size of 20 to 50 nm and the shell thickness of 10 to 30 nm in deionized aqueous solution. These sizes are increased when the samples are created in the polymer solution (see

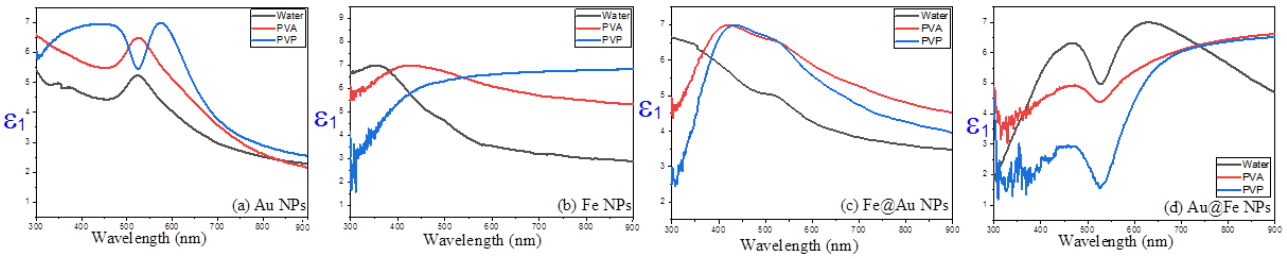

Figure 6. The real dielectric coefficient in terms of wavelength in deionized water compared to the matrix of the PVA and the PVP polymer, for samples (a) Au NPs, (b) Fe NPs, (c) Fe@Au NPs, (d) Au@Fe NPs.

Fig. 5), it can be observed that all the examined samples which formed the core/shell were clearly and distinctly.

3.3 Dielectric properties

It has been realized that the dielectric properties of nanomaterials are very important and play a key role in the position and intensity of the SPR peak of plasmonic NPs. As it is expected, the metal-plasmonic coupling with ferromagnetic metals leads to the change in the refractive index of the samples. The real ε' and imaginary ε'' parts of the relative permittivity are given by

$$\varepsilon' = n^2 - k^2 \quad (1)$$

$$\varepsilon'' = 2nk \quad (2)$$

here n and k are the real and imaginary parts of the refractive index, respectively. (is called extinction factor in literature) and was achieved by Kramers Kronig relationship.

Fig. 6 displays the real parts of the Au NPs, the Fe NPs, and the core-shell refractive index used in this work, it can be clearly noticed that when the gold nanoparticles are excised in the aqueous matrix, we have a distinct peak in the resonance spectrum in the dielectric constant pattern as a guide to the refractive index. But this peak becomes more distinct when used the PVA instead of deionized water. When the PVP is used as a host medium for nanoparticles, a large fundamental change occurs in the real part of the refractive index compared to the deionized water and the PVA (see Fig. 6(a)). This change can be described by the fact that PVP greatly supports the improvement of the localized surface plasmon intensity and location, which confirms that the size obtained with the PVP polymer matrix is the right size to form the plasmon in the best possible form in our work for gold nanoparticles. For the Fe NPs, since it is a non-plasmonic metallic material, there is no characteristic peak in the true refractive index curve (see Fig. 6(b)), where the three curves in the figure indicate a change in the dielectric properties and the real part of refractive index, albeit slight, depending on the host medium used, and this supports configure different sizes when changing the type of ambient medium.

As expected, the coupling between the plasmonic and magnetic metal changed the dielectric coefficients and in turn changed the refractive index of the samples. Here, it is necessary to refer to an essential point, and it is done by comparing the two Figs 6(c) and 6(d), where we note that the real dielectric coefficient of the nanoparticle Au@Fe is much better than that of Fe@Au. The reason is that the presence of gold on the cover increases the property of plasmonic, while when gold is at the core and iron is the cover leads to the extinguishing of the plasmonic feature.

Fig. 7 discusses the imaginary insulating properties as a function of the refractive index, which gives a clearer picture of the surface plasmon behavior. It can be seen as a fundamental change in the imaginary part of the refractive index, although there is a correlation with the real part of the refractive index where they complement each other. This change can be described in (Fig. 7(a)) for three different host mediums. It also noticed an increase in the dielectric properties of iron by change the surrounding medium from deionized water to PVA and then to PVP, (see Fig. 7(b)).

Moreover, the refractive index of the Au@Fe NPs is very different from the refractive index of the Fe@Au NPs, due to the presence of gold once in the shell, which strengthens the surface plasmon phenomenon and again in the core, which leads to the suppression of this phenomenon (see Fig. 7(c,d)). These results are supported by [22].

Table 1. Magnetic properties of core-shell nanoparticles in different solutions.

Samples	Coercive Field (Hc (Oe))	The remanence magnetization Mr (e.m.u/gr)	The saturation magnetization Ms (e.m.u/gr)	The quareness ratio SQR =Mr/Ms
Fe@Au in water	9	1	13	0.077
Fe@Au in PVA	16	1.3	9	0.144
Fe@Au in PVP	65	2	8	0.25
Au@Fe in water	13	1.2	17	0.07
Au@Fe in PVA	32	1.8	11	0.163
Au@Fe in PVP	86	3	10	0.3

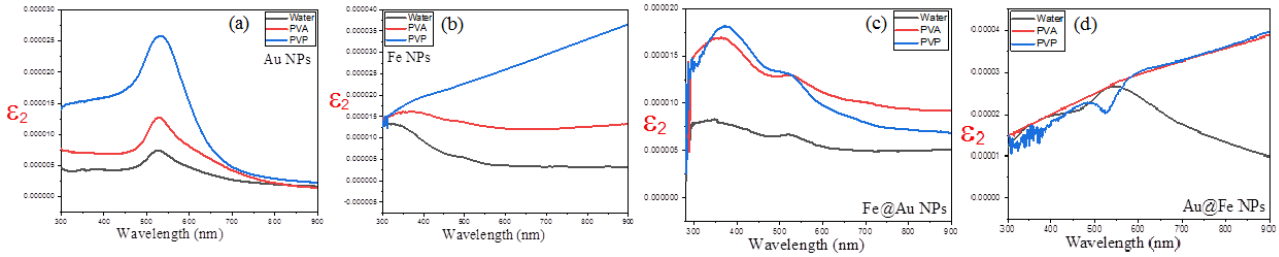

Figure 7. Imaginary dielectric coefficient in terms of wavelength in the deionized water compared to the matrix of PVA and PVP polymers, for samples (a) Au NPs, (b) Fe NPs, (c) Fe@Au NPs, (d) Au@Fe NPs.

3.4 Magnetic properties

In this section, the results of magnetic measurements obtained by shaking samples in a variable magnetic field (VSM device), under an external magnetic field of up to 1 Tesla, will be discussed. A change in the magnetic states of the nanomaterials used in this work was achieved by changing the composition of the core-shell nanomaterials, as well as the surrounding medium. Fig. 8(a) shows the magnetic hysteresis loops of the Fe@Au NPs in deionized water and both PVA and PVP at room temperature (300 K). VSM measurements were performed three weeks after sample synthesis during which it was stored under normal laboratory conditions. All Fe@Au samples showed superparamagnetic behavior in an aqueous matrix with the required field for saturation around (5000 Oe) and approximately (6000 Oe) for polymeric matrix. Although the behavior of the Fe@Au sample in the PVP matrix was changed to a semi-super ferromagnetic behavior, it remains within the superparamagnetic field because the forced magnetic field is very small. This behavior can be justified by the fact that the increase in core size and shell thickness of the samples in the PVP matrix increases the amount of magnetic material present in a single nanostructure, which leads to an increase in all magnetic properties of the sample. Similarly, Fig. 8(b) shows hysteresis loops of Au@Fe nanoparticles in deionized water, both PVA and PVP, at room temperature (300 K).

By comparing the samples Au@Fe and Fe@Au, it is noticed that Au@Fe has a greater magnetization, as the iron in the outer shell of nanoparticles enhances the magnetic properties compared to gold, which dampens the magnetic properties if it is in the shell layer. The PVP polymer also enhanced the magnetic properties compared to the PVA polymer, which indicates that the PVP polymer has better stability by retaining the nanomaterials that are suspended without sedimentation, and this was confirmed previously when examining the optical properties. The magnetic properties of all samples have been summarized in Table 1.

Based on the results, superior magnetic properties are available in core-shell nanoparticles by changing the surrounding medium or changing the composition of samples. In addition, the field magnetization of the agents was increased in the PVP matrix compared to that of the water and polymer PVA matrix. The results could open new insights for researchers into the visible plasmonic-optical effects of photovoltaics.

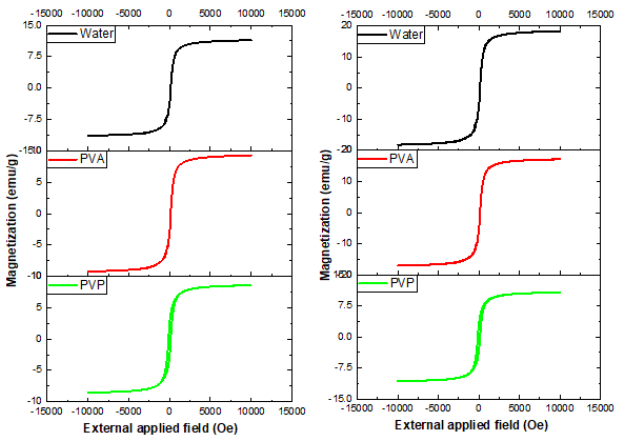

Figure 8. Magnetic behavior of samples Fe@Au and Au@Fe in three different solutions

4. Conclusion

In this study, the Au and the Fe NPs as well as the Au@Fe NPs and the Fe@Au NPs dispersed in different environments were synthesized by laser ablation method, through a comprehensive study of these nanomaterials and in three different solutions, the following conclusions were reached: The results demonstrated there is large tenability and modulation of the SPR absorption band for each group of observed nanomaterial's that may be useful in the design of optical absorber devices. Also the SPR peak is sharper in the PVP matrix due to the properties of the PVP which make it more stable than the aqueous medium. Our results revealed that in the core-shell samples, two distinct peaks can be observed that come from the absorption of each material in the nanostructure. Based on this fact that the core diameter and the shell thickness depended on the surrounding media, it was found that solvents have a significant effect on the linear optical and magnetic properties of the samples. Moreover, the coercieve forced field of the samples is increased in the PVP matrix compared to the water matrix because the main coverage of the polymer over the NPs matrix. In addition, the results showed that the samples have superior magnetic properties that can be modified and controlled by forming the nanomaterials in an appropriate way.

Conflict of interest statement:
The authors declare that they have no conflict of interest.

References

[1] Jeevanandam, Jaison, Ahmed Barhoum, Yen S. Chan, Alain Dufresne, and Michael K. Danquah. "Review on nanoparticles and nanostructured materials: history, sources, toxicity and regulations". *Beilstein Journal of Nanotechnology*, **9**:1050, 2018.

[2] V. Ghorbani and D. Dorranian. "Properties of TiO_2/Au nanocomposite produced by pulsed laser irradiation of mixture of individual colloids". *Applied Physics A*, **122**:1019, 2016.

[3] Daliya S. Mathew and Ruey-Shin Juang. "An overview of the structure and magnetism of spinel ferrite nanoparticles and their synthesis in microemulsions". *Chemical Engineering Journal*, **129**:51, 2007.

[4] H. Nasiri, D. Dorranian, and A. H. Sari. "Green laser assisted gold-iron oxide nanocomposite production". *Radiation Effects and Defects in Solids*, **177**:277, 2022.

[5] S. Khizar, N. M. Ahmad, N. Zine, N. Jaffrezic-Renault, A. Errachid el salhi, and A. Elaissari. "Magnetic nanoparticles: from synthesis to theranostic applications". *ACS Applied Nano Materials*, **4**:4284, 2021.

[6] Vnessa F. Cardoso, A. Francesko V, C. Ribeiro, M. Bañobre-López, P. Martins, and S. Lanceros-Mendez. "Advances in magnetic nanoparticles for biomedical applications". *Advanced Healthcare Materials*, **7**:1700845, 2017.

[7] S. Gul, Sher B. Khan, Inayat U. Rehman, Murad A. Khan, and M. I. Khan. "A comprehensive review of magnetic nanomaterials modern day theranostics"". *Frontiers in Materials*, **6**, 2019.

[8] F. Ahmad, Mounir M. Salem-Bekhit, Faryad Khan, S. Alshehri, Amir Khan, Mohammed M. Ghoneim, H-F Wu, Ehab I. Taha, and I. Elbagory. "Unique properties of surface-functionalized nanoparticles for bio-application: functionalization mechanisms and importance in application". *Nanomaterials*, **12**:1333, 2022.

[9] S. Neveu, A. Bee, M. Robineau, and D. Talbot. "Size-selective chemical synthesis of tartrate stabilized cobalt ferrite ionic magnetic fluid". *Journal of Colloid and Interface Science*, **255**:293, 2002.

[10] J. Szajnar, M. Stawarz, T. Wróbel, and W. Sebzda. "Influence of selected parameters of continuous casting in the electromagnetic field on the distribution of graphite and properties of grey cast iron". *Archives of Metallurgy and Materials*, **59**:747, 2014.

[11] S. Lafon, Irina N. Sokolik, Jean L. Rajot, S. Caquineau, and A. Gaudichet. "Characterization of iron oxides in mineral dust aerosols: Implications for light absorption". *Journal of Geophysical Research*, **111**, 2006.

[12] Fernando M. Melo, Alceu T. Silveira, Lucas F. Quartarolli, Felipe F. Kaid, Daniel R. Cornejo, and Henrique E. Toma. "Magnetic behavior of superparamagnetic nanoparticles containing chelated transition metal ions". *Journal of Magnetism and Magnetic Materials*, **487**:165324, 2019.

[13] N. Sounderya and Y. Zhang. "Use of Core/Shell Structured Nanoparticles for Biomedical Applications". *Recent Patents on Biomedical Engineeringe*, **1**:34, 2008.

[14] H. Mbarak, A. K. Kodeary, S. M. Hamidi, E. Mohajarani, and Y. Zaatar. "Control of nonlinear refractive index of AuNPs doped with nematic liquid crystal under external electric field". *Optik*, **198**:163299, 2019.

[15] H. Chen, L. Zhang, M. Li, and G. Xie. "Synthesis of core–shell micro/nanoparticles and their tribological application: A review". *Materials*, **13**:4590, 2020.

[16] H. Zhou, F. Zou, K. Koh, and J. Lee. "Multifunctional Magnetoplasmonic Nanomaterials and Their Biomedical Applications". *Journal of Biomedical Nanotechnology*, **10**:2921, 2014.

[17] A. K. Kodeary, S. M. Hamidi, and R. Moradlou. "Voltage controlled properties of piezo-magneto-plasmonic core/shell nanoparticles". *Nano-Structures and Nano-Objects*, **21**:100415, 2020.

[18] A. K. Kodeary, M. A. Gatea, S. F. Haddawi, and S. M. Hamidi. "Tunable thermo-piezo-plasmonic effect on core/shell nanoparticles under laser irradiation and external electric field". *Optical and Quantum Electronics*, **52**, 2020.

[19] K. C. Hsieh, H. L. Chen, D. H. Wan, and J. Shieh. "Active Modulation of Surface Plasmon Resonance Wavelengths by Applying an Electric Field to Gold Nanoparticle-Embedded Ferroelectric Films". *The Journal of Physical Chemistry C*, **112**:11673, 2008.

[20] Sanjit M. Majhi, Gautam K. Naik, H-J. Lee, H-G. Song, C-R. Lee, I-H Lee, and Y-T. Yu. "Au@NiO core-shell nanoparticles as a p-type gas sensor: Novel synthesis, characterization, and their gas sensing properties with sensing mechanism". *Sensors and Actuators B: Chemical*, **268**:223, 2018.

[21] M. Heinz, V. V. Srabionyan, L. A. Avakyan, A. L. Bugaev, A. V. Skidanenko, S. Y. Kaptelinin, J. Ihlemann, and et al. "Formation of bimetallic gold-silver nanoparticles in glass by UV laser irradiation". *Journal of Alloys and Compounds*, **767**:1253, 2018.

[22] M. A. Gatea and H. A. Jawad. "Thermoplasmonic of Single Au@SiO_2 and SiO_2@Au Core Shell Nanoparticles in Deionized Water and PolyvinylpyrrolidoneMatrix". *Baghdad Sci. J*, **16**, 2019.

[23] A. K. Kodeary and S. M. Hamidi. "Tunable Piezophotonic Effect on Core-Shell Nanoparticles Prepared by Laser Ablation in Liquids under External Voltage". *Journal of Nanotechnology 2019*, **2019**, 2019.